Protein-Templated Reactions Using DNA-Antibody Conjugates

Lorena Baranda Pellejero, Minke A. D. Nijenhuis, Francesco Ricci and Kurt V. Gothelf**

L. B. Pellejero, Prof. F. Ricci
Department of Chemistry, University of Rome, Tor Vergata
Via della Ricerca Scientifica, 00133 Rome (Italy)
E-mail: francesco.ricci@uniroma2.it

M. A. D. Nijenhuis, Prof. K. V. Gothelf
Department of Chemistry and Interdisciplinary Nanoscience Centre (iNANO)
Aarhus University, Gustav Wieds Vej 14, 8000 Aarhus (Denmark)
E-mail: kvg@inano.au.dk

Keywords: DNA templated reactions, proteins, proximity effect, bioconjugation, nanotechnology

DNA-templated chemical reactions have found wide applications in drug discovery, programmed multistep synthesis, nucleic acid detection and targeted drug delivery. The control of these reactions has, however, been limited to nucleic acid hybridization as a means to direct the proximity between reactants. In this work we introduce a system capable of translating protein-protein binding events into a DNA-templated reaction which leads to the covalent formation of a product. We achieve protein-templated reactions by employing two DNA-antibody conjugates that are both able to recognize the same target protein and to colocalize a pair of reactant DNA strands able to undergo a click reaction. We engineered two individual systems each responsive to human serum albumin (HSA) and human IgG and we demonstrated that, while no reaction occurs in the absence of proteins, both protein-templated reactions can occur simultaneously in the same solution without any inter-system crosstalk.

1. Introduction

DNA-templated chemistry exploits the sequence-specific hybridization of DNA/RNA sequences to control the reactivity of functional groups covalently attached to nucleic acid strands.[1,2] The ability to encode chemical reactions in nucleic acids has enabled the translation of DNA/RNA cues into the formation of different products such as small molecules, signaling moieties and bioactive species.[3,4] Taking advantage of the high programmability of nucleic acids, multistep DNA-templated reactions

have been for example employed to synthesize DNA-encoded libraries containing a large number of possible drug candidates.[5–10]Autonomous systems that are able to achieve multistep DNA-templated synthesis of oligomers or macrocycles have also been demonstrated.[4,11–15] In addition to these applications, DNA-templated reactions have been employed for the detection of specific DNA/RNA target sequences by using templated reactions generating measurable signals, such as fluorogenic reactions or cleavage reactions of quencher molecules that restore the fluorescence.[16–20] Finally, DNA-templated chemistry has found applications in drug-delivery by engineering templated reactions that, upon interaction with a target nucleic acid sequence, can trigger the release of a bioactive molecule.[3,21,22]

For the purpose of templated chemical reactions, synthetic DNA/RNA strands offer several advantages including the spatial control of the reactive groups given by sequence specificity, ability to program multi-step synthesis, and well-established and low-cost synthesis methods. Apart from these important advantages, synthetic DNA can also be used as a versatile molecular scaffold to conjugate different species, a feature that allows to expand the range of molecular cues that can be integrated with DNA-based systems.[23] We recently exploited this feature to control DNA-templated reactions with antibodies by using synthetic DNA strands conjugated to different small molecules and short peptides used as antibody recognition elements.[24]

Thanks to the progress achieved in bioconjugation methods,[23] it is also possible to efficiently conjugate to synthetic DNA strands not only small molecules but also antibodies and proteins. For instance, DNA-antibody conjugates have been established as powerful tools in sensing technologies such as the proximity ligation assay[25] or immuno-PCR[26], in fluorescence microscopy[27] and in super-resolution DNA-PAINT imaging[28], and for the precise spatial arrangement of biomolecules on DNA nanostructures.[29,30] More specifically, the strategy for proximity ligation assay makes use of DNA-antibody conjugates as recognition elements for proteins to trigger an enzymatic amplification.

Inspired from the above-mentioned strategy, we here propose a related design for the use of proteins as cues to direct DNA-templated reactions via a proximity effect by using DNA-antibody conjugates. The strategy allows to widen the class of molecular inputs that can control DNA-templated reactions by introducing the use of proteins as templates. With this approach the reaction toolbox compatible with DNA-templated chemistry will become readily available in a protein-templated fashion, which sets the ground to enable the generation of any type of chemical moiety, such as an imaging or therapeutic agent, upon the presence of specific protein biomarkers.

2. Results and Discussion

2.1. Design for Protein-Templated Reactions

Herein, we propose a design for programmable protein-templated reactions using DNA-antibody conjugates (**Figure 1**). Our approach aims to translate the protein recognition by antibodies to DNA-templated chemistry. The approach employs two DNA-antibody conjugates that are both able to recognize the same target protein and through the appended DNA strands they are able to bind a pair of modified DNA strands (reactant strands), which present a complementary domain and bear reactive groups at their ends. The complementary domain is designed so that the reactant strands do not form a duplex under the diluted conditions employed. Conversely, the bivalent protein-antibody interaction triggers the proximity-induced hybridization of the reactant strands. This ultimately results in an efficient colocalization of the reactive groups which in turn enables their reaction and generation of the chemical product (Figure 1).

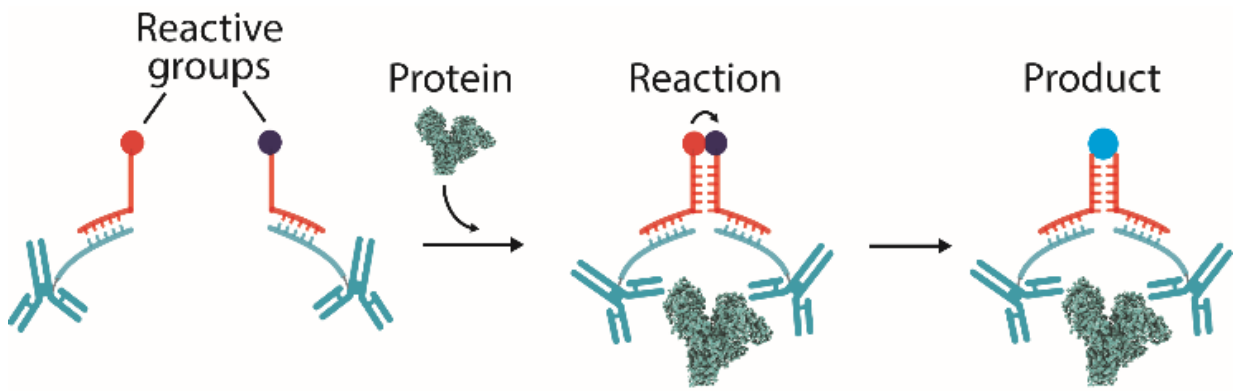

Figure 1. Strategy to achieve protein-templated reactions using DNA-antibody conjugates. Two complementary (10-bp) DNA strands (reactant strands, shown in red) are each conjugated at one end with a reactive group and at the other end they hybridize to a complementary (23-bp) DNA strand on an DNA-antibody conjugate (shown in blue). At low oligonucleotide concentrations (nM), duplex formation between the reactant strands is not favored and thus the reaction rate between the two reactive groups is negligible. Binding of the conjugates to different epitopes on the specific target protein dramatically increases the effective concentration of the reactant DNA strands. This protein-induced proximity effect enables the hybridization of the reactant strands followed by their reaction and subsequent formation of product. The scheme depicted is a simplified version (for the detailed design see Figure S1 in the Supporting Information).

2.2. Site-Directed Labeling of Antibodies

As a first step, we selected human serum albumin (HSA) as the target protein. As HSA-recognizing antibody we employed polyclonal antibodies which are capable of recognizing different epitopes on the

HSA. To synthesize the DNA-antibody conjugate we used a so-called LDLR reagent for site-directed labelling reaction that preferentially targets the hinge region of the antibody to insert an azide handle (**Figure 2**a).[31,32] The azide-labelled antibody was then submitted to further conjugation with a dibenzocyclooctyne (DBCO)-modified DNA sequence. A strain-promoted azide-alkyne cycloaddition (SPAAC) reaction yielded the DNA-antibody construct (Figure 2b and S2). The mono-labelled conjugate was isolated via purification by anion exchange chromatography using a salt gradient (Figure 2c).

2.3. Proximity Induced by Protein

To study the effect of the proximity induced by HSA, we first employed reactant strands labeled with Cy3 and Cy5 fluorophores in place of the reactive groups. This allows us to monitor the HSA-induced colocalization by fluorescence resonance energy transfer (FRET) (Figure 2d). In the presence of HSA, we observed a signal decrease on Cy3 emission due to FRET produced by the colocalization and duplex formation of the reactant strands upon HSA binding to the DNA-antibody conjugates (Figure 2e). The FRET induced by HSA showed a concentration-dependent trend at increasing concentrations of HSA, with an apparent dissociation constant ($K_{1/2}$) of 4.8 ± 0.6 nM (Figure 2f).

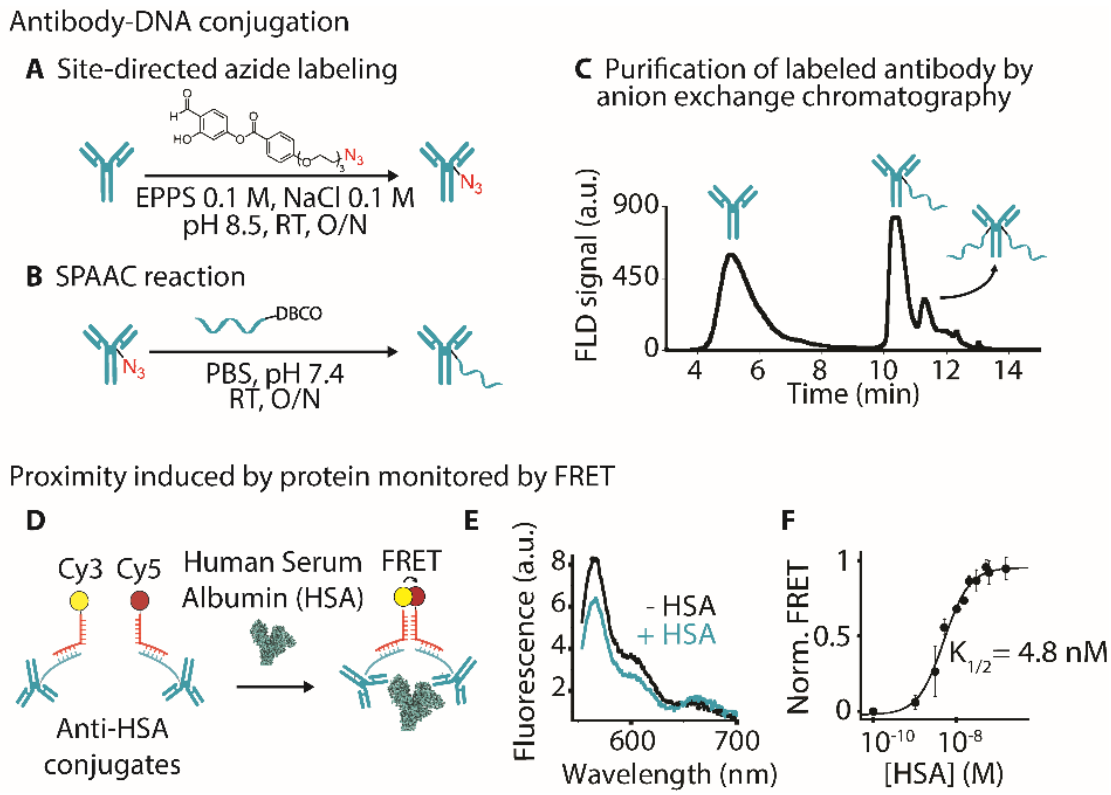

Figure 2. DNA-antibody conjugation and protein-induced proximity monitored by FRET. A) Site-directed labelling of a polyclonal antibody via reaction with a directing reagent bearing an azide handle. B) SPAAC reaction between the labelled antibody and a DBCO-modified DNA strand furnishes the DNA-antibody conjugate. C) Anion exchange chromatogram of the reaction mixture obtained from SPAAC reaction that allows the purification of the monolabelled conjugate. D) Design of a pair of fluorescently labelled DNA strands complementary to anti-HSA conjugates for the study of the proximity effect induced by HSA. E) Fluorescence spectrum of the system shown in (D) in the absence (black) and in the presence of HSA (blue). F) Titration of the system with increasing concentrations of HSA measured by FRET. The $K_{1/2}$ is 4.8 nM. The fluorescence experiments were performed at 37 °C in 25 mM HEPES buffer pH 7.2, 0.1 M NaCl, 0.05% Tween20 at a fixed concentration of the fluorescently labelled strands (30 nM), anti-HSA conjugate (60 nM) in the absence and presence of HSA protein (60 nM, unless otherwise indicated). The experimental values reported in panel (F) represent averages of three independent measurements and the error bars reflect the standard deviations.

2.4. Chemical Reactions Templated by Proteins and Mathematical Model

Motivated by the initial results, we moved to a design containing reactive functional groups at the DNA strands. The two reactant strands are modified with an azide and alkyne group, which are able to undergo a copper-catalyzed azide-alkyne cycloaddition (CuAAC). These reactant strands are again designed to be complementary to the DNA strands on the anti-HSA conjugates to enable modulation of their reaction by HSA (**Figure 3**a). To characterize the resulting product from the reaction, we performed denaturing polyacrylamide electrophoresis (PAGE). We observed that, while no reaction takes place in the absence of HSA, the HSA-templated click reaction does occur at different concentrations of the protein, as evidenced by the visible product band (Figure 3b). The formation of product is dependent on the concentration of HSA. The product formation is reaching a maximum at nearly equimolar concentration of HSA (20 nM) (Figure 3c) and then it is decreasing at higher concentrations. This biphasic trend is similar to what is observed in scaffold proteins that activate signaling pathways by colocalizing other proteins. Such scaffold proteins show in fact an inverted dependence of induced activity at high scaffold concentrations, an effect that is called combinatorial inhibition.[33,34] To demonstrate that the biphasic trend of our protein-templated reaction is governed by the same mechanism we have thus employed a mathematical model previously developed to describe scaffold proteins[35] (see Supporting Information for a full discussion of the model). By adapting this model to our HSA-induced templated reaction, we found that the predicted curve describes the

experimental data quite well (Figure 3c), suggesting that a similar combinatorial inhibition is the cause of the reduced product formation at high HSA concentrations. The increase observed on product formation at larger protein excesses might occur due to protein aggregation which leads to a non-specific colocalization of reactants, in accordance with previous observations.[36]

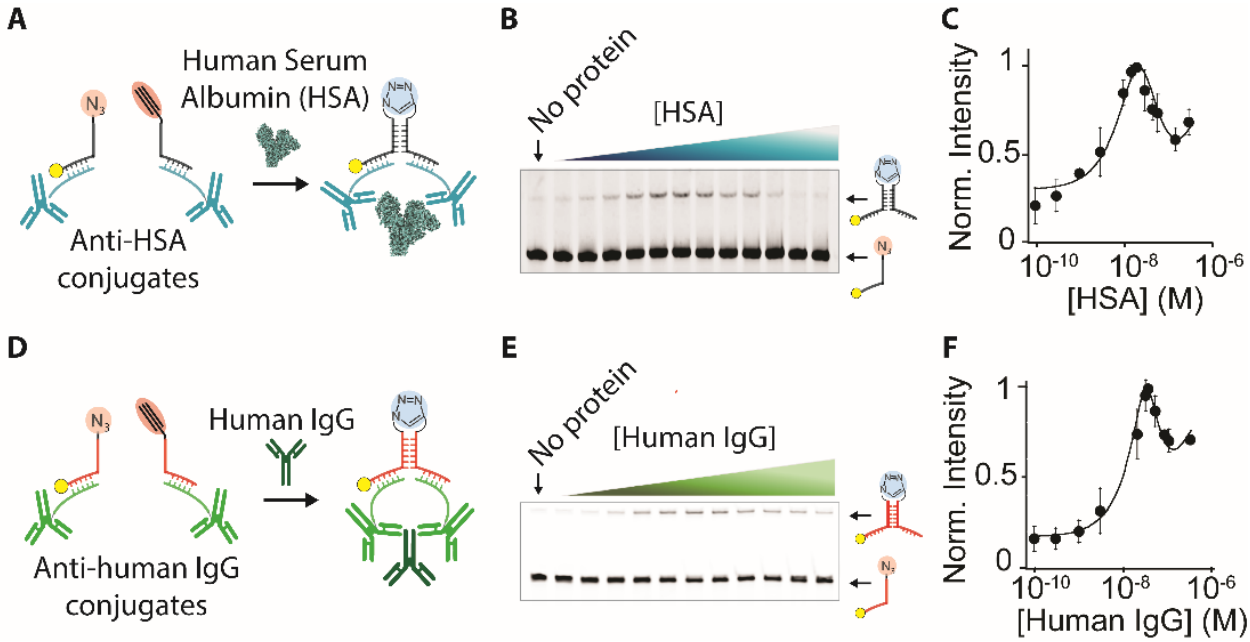

Figure 3. Chemical reactions templated by proteins. A) Scheme of the reaction induced by HSA via the use of anti-HSA conjugates. B) Denaturing PAGE of CuAAC reactions performed at increasing concentrations of HSA. C) Normalized intensity of the product band obtained at increasing concentrations of HSA. D) Scheme of the reaction induced by human IgG antibody via the use of anti-human IgG conjugates. E) Denaturing PAGE of CuAAC reactions performed at increasing concentrations of human IgG. F) Normalized intensity of the product band observed in denaturing PAGE obtained at increasing concentrations of human IgG. Reaction conditions: reactant strands (30 nM), DNA-antibody conjugate (60 nM), protein (either HSA or human IgG, concentration indicated for each case), Cu(I) catalyst (see Supporting Information for details) in 25 mM HEPES buffer pH 7.2, 0.1 M NaCl, 0.05% Tween20. Reactions were run for 30 min at 37 °C. The experimental values reported in panels (C) and (F) represent averages of three independent measurements and the error bars reflect the standard deviations. The mathematical model is represented in (C) and (F) by the solid curve while the experimental points are represented as dots.

A series of control experiments further supports that the reaction is templated by HSA (Figure S3, Supporting Information). A specificity test shows that the system is solely responsive to HSA, as no product is generated in the presence of other proteins (i.e. bovine serum albumin, BSA) (Figure S3, lane

3, Supporting Information). A control experiment in the absence of the anti-HSA conjugate shows no formation of product, which provides further support of the proposed protein-templated reaction (Figure S3, lane 4, Supporting Information). In another control experiment we used a saturating concentration of anti-HSA antibody which competes with the conjugates for the binding of HSA and therefore does not lead to reaction (Figure S3, lane 5, Supporting Information).

The present system displays a high level of modularity, as we can easily tune its responsiveness towards different proteins by changing the nature of the DNA-antibody conjugate. To demonstrate this, we engineered a new system, in this case responsive to human IgG antibodies. We synthesized and purified an anti-human IgG conjugate specific for the Fc region following the previously described bioconjugation method (Figure 2a; Figure S4, Supporting Information). By using Cy3 and Cy5-modified reactant strands, we monitored by FRET their colocalization and duplex formation mediated by human IgG via its protein-protein interaction with the conjugate (Figure S5, Supporting Information). The FRET signal increases at increasing concentrations of human IgG, and we observe a dissociation constant of 6 ± 0.6 Nm (Figure S5, Supporting Information). We then demonstrate that human IgG is able to template the CuAAC click reaction at different concentrations of the colocalizing human IgG, whereas no product is observed in the absence of human IgG (Figure 3e). Similar to the HSA-templated system, the dependency of product formation on human IgG is also in good agreement with simulations from the mathematical model for scaffold proteins. The formation of product increases with human IgG concentration up to a maximum reached at equimolar concentration; it decreases again at excess of human IgG as a result of combinatorial inhibition (Figure 3f). The system shows a high specificity towards human IgG, as no reaction occurs in the presence of other non-specific antibodies (rabbit, sheep and goat IgG) (Figure S6, Supporting Information).

2.5. Orthogonal Protein-Templated Reactions

Complex behavior emerges when multiple concurrent molecular operations with no inter-system interference takes place. Heading towards this, we aim to achieve control of two reactions in the same solution each templated by HSA and human IgG. We use the same design of DNA strands as described and characterized individually above, with the exception that a longer azide-reactant strand is employed in the HSA-responsive system in this case. This provides the two products with different mobilities in gel electrophoresis and thus they are distinguishable (**Figure 4**a). Both HSA and human IgG-responsive systems were tested individually as a control, leading to product formation only in the presence of the corresponding protein for each of the cases, as expected (Figure 4b, lanes 1-4). When employing both systems in the same solution, we observe a similar behavior as when tested individually, which proves that the protein-templated reactions can operate in complex mixtures without cross-reactions (Figure 4b,

lanes 5-7). Lastly, the presence of both HSA and human IgG triggers the corresponding protein-templated reactions in a simultaneous way, evidenced by the two product bands (Figure 4b, lane 8).

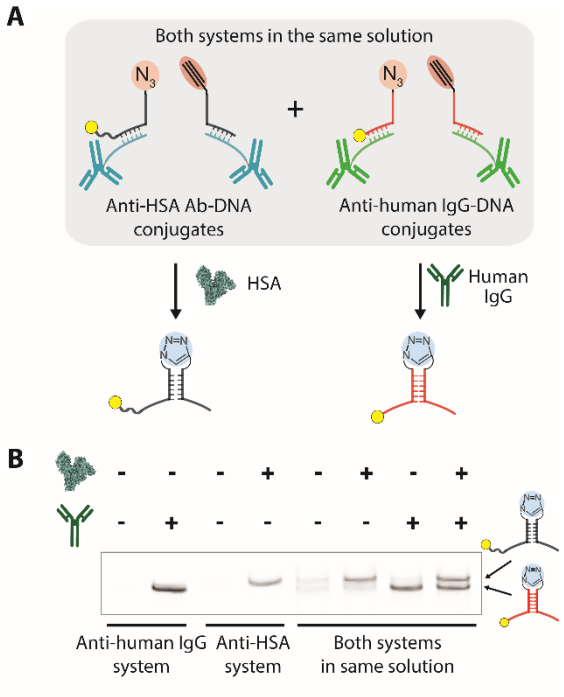

Figure 4. Orthogonal protein-templated reactions. A) Scheme of both systems in the same solution, each of them responsive to a different target protein (either HSA or human IgG). Products from different reactions present slightly different electrophoretic mobilities that makes them distinguishable. B) Denaturing PAGE of CuAAC reactions. First each of the systems is tested individually in the absence and presence of the corresponding protein. Then both systems are tested in the same solution in the absence of proteins, in the presence of one of them and in the presence of both proteins at the same time. Reaction conditions: reactant strands (30 nM), DNA-antibody conjugate (60 nM), protein (either HSA or human IgG, 30 nM), Cu(I) catalyst (see Supporting Information), buffer: 25 mM HEPES buffer pH 7.2, 0.1 M NaCl, 0.05% Tween20. Reactions were run for 30 min at 37 °C.

3. Conclusion

Here, we have demonstrated that the integration of protein-protein interactions and DNA-templated chemistry into the same system can enable orthogonal protein-templated chemical reactions via the use of DNA-antibody conjugates. We engineered a system consisting of two reactant DNA strands bearing reactive groups at their ends that are designed to hybridize to DNA-antibody conjugates. Only upon the presence of the specific protein recognized by the conjugates, the two reactant strands are brought into

close proximity via protein-protein interactions. This protein-mediated colocalization induces the hybridization of the reactant strands enabling their templated reaction and generation of a product.

We designed a reactive system that employs DNA-antibody conjugates to allow for HSA to template a CuAAC reaction, which was characterized by denaturing PAGE. By changing the nature of the DNA-antibody conjugate on the system we demonstrated the same principle with a different protein, i.e. human IgG. The dependency of product formation on the concentration of templating protein was in good agreement with a scaffold protein model. Both systems, each responsive to either HSA or human IgG, could operate in parallel when set in the same solution, showing no crosstalk with one another.

The system developed in this work shows that it is possible to translate protein-protein binding events to a DNA-templated chemical reaction, leaving the covalent product as an independent and permanent signature of the protein-protein interactions. The proposed strategy exploits the available repertoire of antibodies able to recognize specific proteins with high affinity, the colocalization efficiency of the reactants given by both antibody-protein interactions and DNA hybridization, and the possibility to integrate antibodies to DNA constructs via bioconjugation methods. The approach is specific and orthogonal and in principle could be applied to any protein for which antibodies binding to different epitopes are available. We envision that the reported protein-templated reaction could be coupled to downstream processes, for instance by using the click ligated product as template for amplification or transcription, as shown in previous studies.[37] The present strategy may also serve as a general platform to achieve a final step in the synthesis of bioactive therapeutic agents by using other class of chemical reactions templated by specific proteins.

Experimental Section

Experimental Section can be found in the Supporting Information.

Supporting Information

Supporting Information is available from the Wiley Online Library or from the author.

Acknowledgements

The work is funded by the Marie Skłodowska-Curie ITN project DNA-robotics (project n. 765703) (L.B.P., M.A.D.N., F.R., K.V.G.), L'Oréal Italia-UNESCO "For Women In Science" (L.B.P), Novo Nordisk foundation (CEMBID) (Grant Number NNF17OC0028070) (K.V.G.), Associazione Italiana per la Ricerca sul Cancro, AIRC (project n. 21965) (F.R.) and by the European Research Council, ERC (Consolidator Grant project n. 819160) (F.R.).

We would like to thank Anders Märcher (post-doctoral researcher at Kurt Gothelf's group) for supplying the directing reagent for bioconjugation.

Received: ((will be filled in by the editorial staff))
Revised: ((will be filled in by the editorial staff))
Published online: ((will be filled in by the editorial staff))

References

[1] Z. J. Gartner, M. W. Kanan, D. R. Liu, *Angew. Chemie Int. Ed.* **2002**, *41*, 1796–1800.

[2] C. T. Calderone, J. W. Puckett, Z. J. Gartner, D. R. Liu, *Angew. Chemie Int. Ed.* **2002**, *41*, 4104–4108.

[3] K. Gorska, N. Winssinger, *Angew. Chemie - Int. Ed.* **2013**, *52*, 6820–6843.

[4] R. K. O'Reilly, A. J. Turberfield, T. R. Wilks, *Acc. Chem. Res.* **2017**, *50*, 2496–2509.

[5] M. W. Kanan, M. M. Rozenman, K. Sakural, T. M. Snyder, D. R. Liu, *Nature* **2004**, *431*, 545–549.

[6] Z. J. Gartner, B. N. Tse, R. Grubina, J. B. Doyon, T. M. Snyder, D. R. Liu, *Science (80-.).* **2004**, *305*, 1601–1605.

[7] M. H. Hansen, P. Blakskjaer, L. K. Petersen, T. H. Hansen, J. W. Hoøjfeldt, K. V. Gothelf, N. J. V. Hansen, *J. Am. Chem. Soc.* **2009**, *131*, 1322–1327.

[8] L. K. Petersen, P. Blakskjær, A. Chaikuad, A. B. Christensen, J. Dietvorst, J. Holmkvist, S. Knapp, M. Kořínek, L. K. Larsen, A. E. Pedersen, et al., *Medchemcomm* **2016**, *7*, 1332–1339.

[9] R. A. Goodnow, C. E. Dumelin, A. D. Keefe, *Nat. Rev. Drug Discov.* **2017**, *16*, 131–147.

[10] D. L. Usanov, A. I. Chan, J. P. Maianti, D. R. Liu, *Nat. Chem.* **2018**, *10*, 704–714.

[11] M. L. McKee, P. J. Milnes, J. Bath, E. Stulz, A. J. Turberfield, R. K. O'Reilly, *Angew. Chemie* **2010**, *122*, 8120–8123.

[12] Y. He, D. R. Liu, *Nat. Nanotechnol.* **2010**, *5*, 778–782.

[13] P. J. Milnes, M. L. McKee, J. Bath, L. Song, E. Stulz, A. J. Turberfield, R. K. O'Reilly, *Chem. Commun.* **2012**, *48*, 5614–5616.

[14] M. L. McKee, P. J. Milnes, J. Bath, E. Stulz, R. K. O'Reilly, A. J. Turberfield, *J. Am. Chem. Soc.* **2012**, *134*, 1446–1449.

[15] W. Meng, R. A. Muscat, M. L. McKee, P. J. Milnes, A. H. El-Sagheer, J. Bath, B. G. Davis, T. Brown, R. K. O'Reilly, A. J. Turberfield, *Nat. Chem.* **2016**, *8*, 542–548.

[16] Silverman AP, Kool ET, *Chem Rev*. **2006**, *106(9),* 3775-3789.

[17] A. Shibata, H. Abe, Y. Ito, *Molecules* **2012**, *17*, 2446–2463.

[18] C. Percivalle, J.-F. Bartolo, S. Ladame, *Org. Biomol. Chem.* **2013**, *11*, 16–26.

[19] M. Di Pisa, O. Seitz, *ChemMedChem* **2017**, *12*, 872–882.

[20] D. Al Sulaiman, J. Y. H. Chang, S. Ladame, *Angew. Chemie* **2017**, *129*, 5331–5335.

[21] K. T. Kim, S. Angerani, D. Chang, N. Winssinger, *J. Am. Chem. Soc.* **2019**, *141*, 16288–16295.

[22] E. Janett, K. Diep, K. M. Fromm, C. G. Bochet, *ACS Sensors* **2020** *5* (8), 2338-2343.

[23] M. Madsen, K. V Gothelf, *Chem. Rev.* **2019**, *119*, 6384–6458.

[24] L. Baranda Pellejero, M. Mahdifar, G. Ercolani, J. Watson, T. Brown, F. Ricci, *Nat. Commun.* **2020**, *11*, 6242.

[25] O. Söderberg, M. Gullberg, M. Jarvius, K. Ridderstråle, K. J. Leuchowius, J. Jarvius, K. Wester, P. Hydbring, F. Bahram, L. G. Larsson, U. Landegren, *Nat. Methods* **2006**, *3*, 995-1000.

[26] T. Sano, C. L. Smith, C. R. Cantor, *Science,* **1992**, *258*, 120–122.

[27] J. Schwach, K. Kolobynina, K. Brandstetter, M. Gerlach, P. Ochtrop, J. Helma, C. P. R. Hackenberger, H. Harz, M. C. Cardoso, H. Leonhardt, A. Stengl, *Chembiochem* **2021**, *22*, 1205-1209.

[28] G. A. O. Cremers, B. J. H. M. Rosier, R. Riera Brillas, L. Albertazzi, T. F. A. De Greef, *Bioconjug. Chem.,* **2019**, *30*, 2384–2392.

[29] N. Stephanopoulos, *Chem* **2020**, *6*, 364–405.

[30] B. Saccà, C. M. Niemeyer, *Chem. Soc. Rev.* **2011**, *40*, 5910–5921.

[31] A. Märcher, M. A. D. Nijenhuis, K. V Gothelf, *Angew. Chemie Int. Ed.* **2021**, *60*, 21691–21696.

[32] A. Märcher, J. Palmfeldt, M. Nisavic, K. V. Gothelf, *Angew. Chemie - Int. Ed.* **2021**, *60,* 6539–6544.

[33] E. F. Douglass, C. J. Miller, G. Sparer, H. Shapiro, D. A. Spiegel, *J. Am. Chem. Soc.* **2013**, *135*, 6092–6099.

[34] J. J. McCann, U. B. Choi, M. E. Bowen, *Structure* **2014**, *22*, 1458–1466.

[35] A. den Hamer, L. J. M. Lemmens, M. A. D. Nijenhuis, C. Ottmann, M. Merkx, T. F. A. de Greef, L. Brunsveld, *Chembiochem* **2017**, *18*, 331–335.

[36] T. Mashima, B. J. H. M. Rosier, K. Oohora, T. F. A. de Greef, T. Hayashi, L. Brunsveld, *Angew. Chemie - Int. Ed.* **2021**, *60*, 11262–11266.

[37] A. H. El-Sagheer, T. Brown, *Acc. Chem. Res.*, **2012**, *45*, 1258–1267.